



## Reliability Analysis of Composite Steel Column Subjected to Monotonic Loading

### KEYWORDS

ANSYS.12, Buckling Analysis, Finite Element Modelling, Concrete Filled Steel Tube(CFST), Reliability

### Pradeep k

PG Student of Structural Engineering, Department of Civil Engineering, Ghouseia College of Engineering, Ramanagara, Karnataka, India

### khalid Nayaz Khan

Associate Professor, Department of Civil Engineering, Ghouseia College of Engineering Ramanagara, Karnataka, India.

### Dr. N.S Kumar

Professor, Director of R&D, Department of Civil Engineering, Ghouseia College of Engineering Ramanagara, Karnataka, India .

**ABSTRACT** This Research aims to study the behavior of axially loaded hollow steel tube concrete-filled steel tube(CFST) columns under monotonic loading using the finite element software ANSYS.12. Modeling accuracy is established by comparing results of the Nonlinear Analysis and the Experimental test. It is concluded that the parameters have considerable effect on the behaviour of the columns. The prime factors considered to affect ultimate axial load and corresponding axial shortening under axial compression are cross-sectional area (A), wall thickness of the steel tube (t), strength of in-filled concrete (f<sub>cu</sub>). Most of the research on concrete-filled steel tube is restricted to a deterministic approach. To gain clear insight into the random properties of circular concrete-filled steel tube, reliability analysis is carried out in the present study. Materials specifications, resistance model, and load models were designed using structural reliability techniques. the reliability of concrete-filled steel tube was investigated using the first-order reliability method(FORM) combined with nonlinear finite element analysis.

### 1.0 INTRODUCTION

At the present time, the concrete filled steel tube columns are widely used in construction. Actually, this type of structural elements is favored in practice because of its small cross sectional area to load carrying capacity ratio. Hence, mega concrete columns in tall buildings' lower floors can be substituted by smaller sections of CFST columns. Moreover, CFST elements can be used as piers for bridges at congested areas. Therefore, such structural elements should be thoroughly investigated before used in critical structures. Concrete filled tubular (CFT) columns combine the action of steel and concrete when carrying compression loads and moments showing an ideal structural performance. While the steel tube confines the concrete core enhancing its compressive strength, the concrete core prevents the steel section from experiencing local buckling. Due to that, the use of CFT columns has increased, becoming very popular in the last years.

Composite columns comprise a combination of concrete and steel and utilize the most favorable properties of the constituent materials. Use of composite columns can result in significant savings in column size, which ultimately can lead to considerable economic savings. This reduction in column size provides is particularly beneficial where floor space is at a premium, such as in car parks and office blocks. The use of stainless steel columns filled with concrete is relatively new and innovative, and not only provides the advantages outlined above but also brings the durability associated with stainless steel. The term 'composite column' refers to a compression member in which the steel and concrete elements act compositely. The role of the concrete core in a composite column is not only to resist compressive forces but also to reduce the potential for buckling of the steel member. The steel tube reinforces the concrete to resist any tensile forces, bending moments and shear forces, and offers confinement to the concrete. Composite columns can buckle in local or overall modes, but this investigation is focused on the cross-section resist-

ance of short composite columns, where only local buckling effects were exhibited. In current international practice, concrete-filled steel tube (CFT) columns are used in the primary lateral resistance systems of both braced and un-braced building structures. There exist applications in Japan and Europe where CFTs are also used as bridge piers. Moreover, CFT's may be utilized for retrofitting purposes for strengthening concrete columns in earthquake zones.

### 1.2 Structural Behavior

The interaction between the steel tube and the concrete core is the key issue for understanding the behavior of concrete-filled steel tube columns. Since steel and concrete are two materials with different stress-strain curves, determination of the effective structural property of a CFT element becomes a difficult task. The important parameters affecting the load-deformation behavior, the ultimate strength and the failure mechanism of CFTs under a given loading condition are;

- The geometric parameters like shape of the cross section, member size, thickness of steel tube, L/B ratio of the tube.
- Grades of concrete and steel
- Type and rate of application of loading and boundary condition

## 2.0 FINITE ELEMENT METHOD

### 2.1 INTRODUCTION

The basic concept in the physical interpretation of the FEM is the subdivision of then mathematical model into disjoint (non-overlapping) components of simple geometry called finite elements. The finite element method is a numerical analysis technique for obtaining approximate solutions to a wide variety of engineering problems. ANSYS is a general purpose finite element modeling package for numerically solving a wide variety of problems which include static/dynamic structural analysis (both linear and nonlin-

ear), heat transfer and fluid problems, as well as acoustic and electro-magnetic problems. The mechanical buckling have been analyzed using a finite element (FE) model in ANSYS. The basic concept of finite element method is discretization of a structure into finite number of elements, connected at finite number of points called nodes. The material properties and the governing relationships are considered over these elements and expressed in terms of nodal displacement at nodes. The response of each element is expressed in terms of a finite number of degrees of freedom characterized as the value of an unknown function, or functions, at a set of nodal points. The finite element method model is then considered to be approximated by that of the discrete model obtained by connecting or assembling the collection of all elements. The disconnection-assembly concept occurs naturally when examining many artificial and natural systems. For example, it is easy to visualize an engine, bridge, building, airplane, or skeleton as fabricated from simpler components. Unlike finite difference models, finite elements do not overlap in space

**2.2 Elements Used**

Two main types of Elements are considered in the proposed FE modeling of CFST. Concrete infill is modeled using solid64 element whereas the steel tube is modeled using shell181 element used

**2.2.1 Shell181**

SHELL181 is suitable for analyzing thin to moderately-thick shell structures. It is a four-node element with six degrees of freedom at each node: translations in the x, y, and z directions, and rotations about the x, y, and z-axes. (If the membrane option is used, the element has translational degrees of freedom only). The degenerate triangular option should only be used as filler elements in mesh generation. SHELL181 is well-suited for linear, large rotation, and/or large strain nonlinear applications. Change in shell thickness is accounted for in nonlinear analyses. In the element domain, both full and reduced integration schemes are supported. SHELL181 accounts

For follows (load stiffness) effects of distributed pressures SHELL181 accounts for follower (load stiffness) effects of distributed pressures.

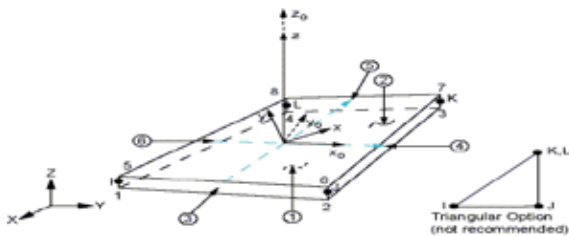


Figure 2.1: Shell 181 Geometry

**2.2.2 Concrete 65**

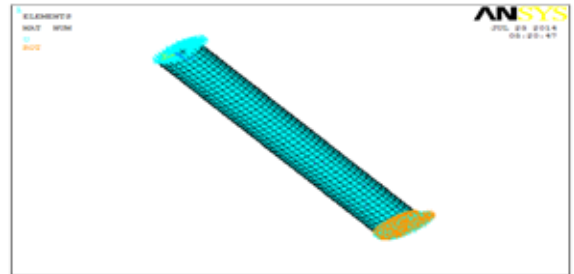
SOLID65 is used for the three-dimensional modeling of solids with or without reinforcing bars (rebars). The solid is capable of cracking in tension and crushing in compression. In concrete applications, for example, the solid capability of the element may be used to model the concrete while the rebar capability is available for modeling reinforcement behavior. Other cases for which the element is also applicable would be reinforced composites and geological materials. The element is defined by eight nodes having three degrees

**2.3 Boundary Conditions**

The two ends were considered to be hinged (Fig ) for modeling. Both the ends, displacement degrees of freedom in x, y directions ( $U_x, U_y$ ) were restrained and translation  $U_z$  as well as rotational degrees of freedom in x, y, z directions ( $\Theta_x, \Theta_y,$  and  $\Theta_z$ ) was considered to be free.

**2.4 Specimen Geometry**

All modeling was conducted using ANSYS 12 finite element software. The project proceeded in several stages of modeling; hollow specimens were modeled as 3D shell181 and concrete specimens were modeled as solid65 element with identical geometry. The dimensions of the sections were chosen to match those being used in the experimental testing of the experiment



**2.5 Material Specification**

**Steel**

- a) Material : Structural Steel Fe 310 Mpa
- b) Young's Modulus  $E=200Gpa$
- c) Poisson's ratio =0.3
- d) Density =7850kg/m<sup>3</sup>.

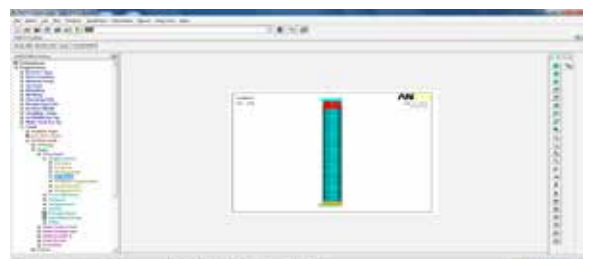
**Concrete**

- a) Grade of Concrete:M20/M25/M30
- b) Young's Modulus  $E=22360.67Mpa/2500Mpa/27386.12 Mpa$
- c) Poisson's ratio = 0.2
- d) Density=2400kg/m<sup>3</sup>

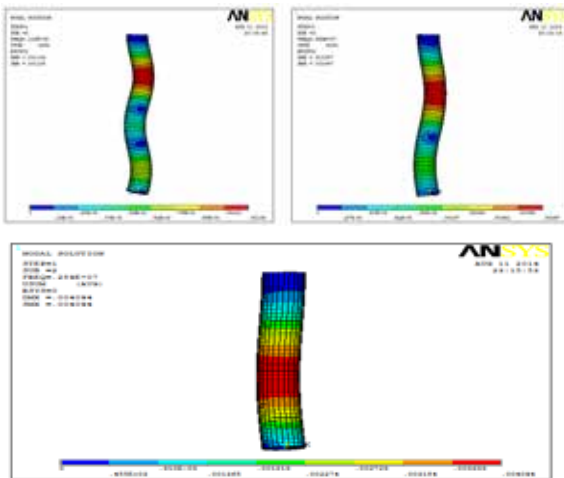
**1) Meshing The Solid Volume And Extrude The Volume To a Given Length ( 5mm size of mesh)**



**2) Applying The force And Displacement on Nodes of Concrete Filled Steel Tube**



3) Modes Shapes of Concrete Filled Steel Tube Column



3.0 RELIABILITY ANALYSIS

3.1 Reliability Definition

Reliability might be defined as the probability that a structural system will survive the given load level. There is a counter part to reliability called probability of failure (Pf). It is defined as the probability that a structural system will fail under the given loading conditions. Hence, reliability and probability of failure form two extremes related to the safety of structural systems. Probability theory states that the sum of reliability and probability of failure is always equal to unity. This rule makes it easy to evaluate one quantity if the other one is known

3.2 The first-order reliability method (FORM)

Approaches such as the Monte Carlo method, importance sampling method, FORM, and the second-order reliability method (SORM), are intensively used in structural reliability analysis. Generally, the failure probability can be written as

$$Pf = \int_{g(x) \leq 0} f_x(x) dx$$

where X is the vector of random variables,  $f_x(x)$  denotes the joint probability density function of X, and  $g(x)$  is the limit state function. For reliability analysis by FORM, the basic random variables must be transformed in to the uncorrelated standard normal space by  $Y=Y(X)$ . Then, above Eq is rewritten.

$$Pf = \int_{G(Y) \leq 0} \Phi(Y) dy$$

where  $\Phi$  is the standard normal density of Y and  $G(Y)$  is the limit state function in an uncorrelated standard normal space. Then, on the limit-state surface  $G(Y)=0$ , the point that has the minimum distance to the origin will be found. This point is named as the design point, which has the highest likelihood of being in the failure domain and makes the dominant contribution to the failure integral. The corresponding first-order estimate of failure probability is  $Pf = \Phi(-\beta)$  where  $\beta$ , the reliability index, is the distance between the origin and design point.

The reliability index,  $\beta$ , can be defined as the safety index. Then, the reliability index can be calculated from Cornell (1967, 1969) as

$$\beta = \frac{\mu_R - \mu_S}{\sqrt{\sigma_R^2 + \sigma_S^2}}$$

Analytical Results of CFST Using ANSYS And Comparison With Experimental Results

Sl no.	Diameter (mm)	Thickness (mm)	Length (mm)	D/t Ratio	L/D Ratio	Grades of Concrete	$f_y$ (N/mm <sup>2</sup> )	% of Epoxy	Ultimate Load Pu Experimental	Ultimate Load Pu Using ANSYS (kN)	EUROCODE 4 $NEC4=A_s^*f_y+A_c^*f_c$	ACI method, $NACI=A_s^*f_y+0.85*A_c^*f_c$	BS5400 method, $NBS5400=A_s^*f_y + 0.675*A_c^*f_c$
1	60.3	2.90	301.5	20.79	5	20	310	-	199.10	196.77	216.19	209.33	201.20
2	60.3	3.60	301.5	16.75	5	20	310	-	224.82	219.08	242.95	236.31	228.57
3	60.3	4.50	301.5	13.40	5	20	310	-	250.63	245.88	285.73	279.53	272.30
4	60.3	2.90	422.1	20.79	7	20	310	-	194.72	189.68	216.19	209.33	201.20
5	60.3	3.60	422.1	16.75	7	20	310	-	206.31	203.29	242.95	236.31	228.57
6	60.3	4.50	422.1	13.40	7	20	310	-	230.12	225.53	285.73	279.53	272.30
7	60.3	2.90	542.7	20.79	9	20	310	-	179.52	175.42	216.19	209.33	201.20
8	60.3	3.60	542.7	16.75	9	20	310	-	199.40	193.35	242.95	236.31	228.57
9	60.3	4.50	542.7	13.40	9	20	310	-	219.20	215.12	285.73	279.53	272.30
10	60.3	2.90	301.5	20.79	5	25	310	-	207.07	203.10	227.70	218.96	208.87
11	60.3	3.60	301.5	16.75	5	25	310	-	232.63	225.02	254.02	245.78	236.08
12	60.3	4.50	301.5	13.40	5	25	310	-	259.82	256.50	296.06	288.16	279.27
13	60.3	2.90	422.1	20.79	7	25	310	-	204.13	201.20	227.70	218.96	208.87
14	60.3	3.60	422.1	16.75	7	25	310	-	220.73	215.93	254.02	245.78	236.08
15	60.3	4.50	422.1	13.40	7	25	310	-	248.09	242.17	296.06	288.16	279.27
16	60.3	2.90	542.7	20.79	9	25	310	-	200.41	196.49	227.70	218.96	208.87

Analytical Results of CFST Using ANSYS And Comparison With Experimental Results

17	60.3	3.60	542.7	16.75	9	25	310	-	208.33	205.73	254.02	245.78	236.08
18	60.3	4.50	542.7	13.40	9	25	310	-	229.51	224.15	296.06	288.16	279.27
19	60.3	2.90	301.5	20.79	5	30	310	-	221.03	215.78	239.14	228.76	216.65
20	60.3	3.60	301.5	16.75	5	30	310	-	233.92	230.80	265.09	255.12	243.50
21	60.3	4.50	301.5	13.40	5	30	310	-	268.16	262.61	306.39	297.09	286.24
22	60.3	2.90	422.1	20.79	7	30	310	-	213.01	210.91	239.14	228.76	216.65
23	60.3	3.60	422.1	16.75	7	30	310	-	230.53	226.18	265.09	255.12	243.50
24	60.3	4.50	422.1	13.40	7	30	310	-	259.12	254.86	306.39	297.09	286.24
25	60.3	2.90	542.7	20.79	9	30	310	-	207.02	201.19	239.14	228.76	216.65
26	60.3	3.60	542.7	16.75	9	30	310	-	214.15	210.59	265.09	255.12	243.50
27	60.3	4.50	542.7	13.40	9	30	310	-	236.22	230.75	306.39	297.09	286.24
46	60.3	2.90	301.5	20.79	5	HOLLOW	310	-	153.12	150.11	170.05	170.05	170.05
47	60.3	3.60	301.5	16.75	5	HOLLOW	310	-	174.01	168.14	198.68	198.68	198.68
48	60.3	4.50	301.5	13.14	5	HOLLOW	310	-	186.12	181.91	204.42	204.42	204.42
49	60.3	2.90	422.1	20.79	7	HOLLOW	310	-	143.71	138.37	170.05	170.05	170.05
50	60.3	3.60	422.1	16.75	7	HOLLOW	310	-	132.17	127.26	198.68	198.68	198.68
51	60.3	4.50	422.1	13.14	7	HOLLOW	310	-	121.12	115.07	204.42	204.42	204.42
52	60.3	2.90	542.7	20.79	9	HOLLOW	310	-	122.03	115.20	170.05	170.05	170.05
53	60.3	3.60	542.7	16.75	9	HOLLOW	310	-	118.53	112.35	198.68	198.68	198.68
54	60.3	4.50	542.7	13.14	9	HOLLOW	310	-	104.17	101.48	204.42	204.42	204.42
55	60.3	2.90	301.5	20.79	5	20	310	2%	206.31	201.17	218.68	215.03	206.35
56	60.3	2.90	301.5	20.79	5	20	310	4%	212.26	208.32	224.56	217.35	211.23
57	60.3	3.60	301.5	16.75	5	20	310	2%	230.34	224.21	223.12	218.39	215.36
58	60.3	3.60	301.5	16.75	5	20	310	4%	232.40	228.92	225.96	221.78	219.87
59	60.3	4.50	301.5	13.40	5	20	310	2%	252.17	248.23	249.89	245.91	241.43
60	60.3	4.50	301.5	13.40	5	20	310	4%	259.11	255.18	253.43	254.68	250.89
61	60.3	2.90	422.1	20.79	7	20	310	2%	198.59	193.65	193.12	188.61	185.64
62	60.3	2.90	422.1	20.79	7	20	310	4%	202.82	197.12	196.87	191.32	187.84
63	60.3	3.60	422.1	16.75	7	20	310	2%	210.49	206.94	205.48	201.55	198.45
64	60.3	3.60	422.1	16.75	7	20	310	4%	216.18	211.03	209.56	205.38	202.52
65	60.3	4.50	422.1	13.40	7	20	310	2%	234.51	228.35	229.65	225.91	223.63
66	60.3	4.50	422.1	13.40	7	20	310	4%	239.60	236.55	233.75	229.54	225.18
67	60.3	2.90	542.7	20.79	9	20	310	2%	184.39	178.63	178.41	175.25	172.33
68	60.3	2.90	542.7	20.79	9	20	310	4%	187.03	182.33	184.15	181.47	178.68
69	60.3	3.60	542.7	16.75	9	20	310	2%	201.53	196.84	196.16	190.71	187.89
70	60.3	3.60	542.7	16.75	9	20	310	4%	208.67	202.21	198.02	194.62	191.52
71	60.3	4.50	542.7	13.40	9	20	310	2%	223.72	219.48	218.19	214.86	213.86
72	60.3	4.50	542.7	13.40	9	20	310	4%	232.01	225.71	229.68	226.45	221.71

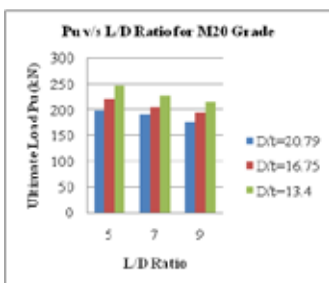


Fig 2.2:Pu v/s L/D Ratio for M20 Grade

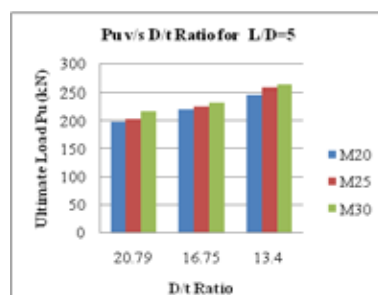


Fig 2.3:Pu v/s D/t Ratio for L/D=5

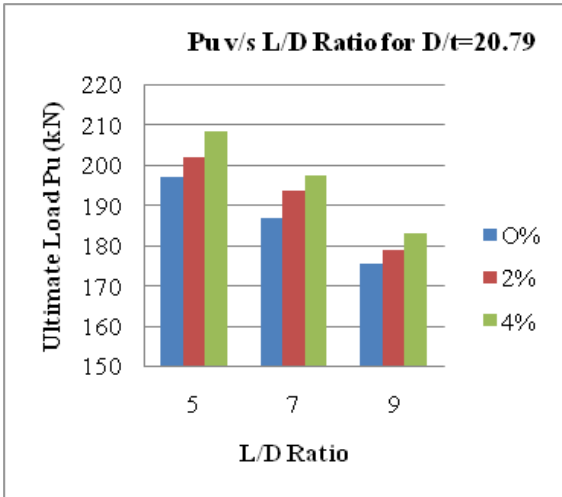


Fig 2.4:Pu v/s L/D Ratio for D/t=20.79

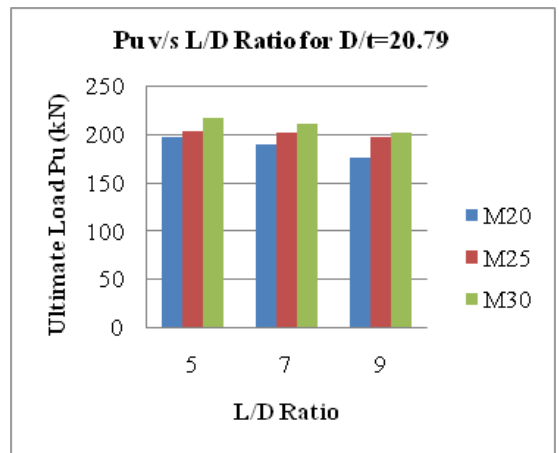


Fig 2.6:Pu v/s L/D Ratio for D/t=20.79

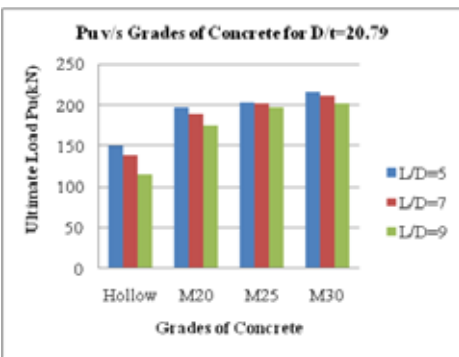


Fig2.5:Pu v/s Grades of Concrete for D/t=20.79

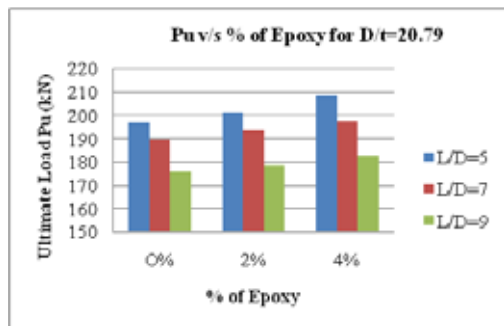


Fig 2.7:Pu v/s % of Epoxy for D/t=20.79

Reliability Index And Probability of Failure For CSFT Column

Sl no.	Diameter (mm)	Thickness (mm)	Length (mm)	D/t Ratio	L/D Ratio	Grades of Concrete	$f_c$ (N/mm <sup>2</sup> )	% of Epoxy	Ultimate Load Pu Using ANSYS (kN)	Reliability Index	Probability of failure $P_f = \Phi(-\beta)$
1	60.3	2.90	301.5	20.79	5	20	310	-	196.77	1.30	0.09680
2	60.3	3.60	301.5	16.75	5	20	310	-	219.08	1.88	0.03005
3	60.3	4.50	301.5	13.40	5	20	310	-	245.88	2.25	0.01222
4	60.3	2.90	422.1	20.79	7	20	310	-	189.68	1.21	0.11314
5	60.3	3.60	422.1	16.75	7	20	310	-	203.29	1.62	0.05262
6	60.3	4.50	422.1	13.40	7	20	310	-	225.53	2.15	0.01578
7	60.3	2.90	542.7	20.79	9	20	310	-	175.42	1.12	0.13136
8	60.3	3.60	542.7	16.75	9	20	310	-	193.35	1.32	0.09342
9	60.3	4.50	542.7	13.40	9	25	310	-	215.12	2.09	0.01831
10	60.3	2.90	301.5	20.79	5	25	310	-	203.10	1.98	0.02385
11	60.3	3.60	301.5	16.75	5	25	310	-	225.02	2.46	0.00695
12	60.3	4.50	301.5	13.40	5	25	310	-	256.50	2.73	0.00317
13	60.3	2.90	422.1	20.79	7	25	310	-	201.20	1.63	0.05155
14	60.3	3.60	422.1	16.75	7	25	310	-	215.93	2.14	0.01618
15	60.3	4.50	422.1	13.40	7	25	310	-	242.17	2.32	0.01017

16	60.3	2.90	542.7	20.79	9	25	310	-	196.49	1.48	0.06944
17	60.3	3.60	542.7	16.75	9	25	310	-	205.73	2.05	0.02018
18	60.3	4.50	542.7	13.40	9	25	310	-	224.15	2.18	0.01463
19	60.3	2.90	301.5	20.79	5	30	310	-	215.78	2.65	0.00402
20	60.3	3.60	301.5	16.75	5	30	310	-	230.80	2.92	0.00175
21	60.3	4.50	301.5	13.40	5	30	310	-	262.61	3.49	0.24
22	60.3	2.90	422.1	20.79	7	30	310	-	210.91	2.45	0.00714
23	60.3	3.60	422.1	16.75	7	30	310	-	226.18	2.51	0.0604
24	60.3	4.50	422.1	13.40	7	30	310	-	254.86	3.15	0.81
25	60.3	2.90	542.7	20.79	9	30	310	-	201.19	2.20	0.01390
26	60.3	3.60	542.7	16.75	9	30	310	-	210.59	2.35	0.01463
27	60.3	4.50	542.7	13.40	9	30	310	-	230.75	2.82	0.00240
28	60.3	2.90	301.5	20.79	5	20	310	2%	201.17	1.92	0.02743
29	60.3	2.90	301.5	20.79	5	20	310	4%	208.32	2.18	0.01463
30	60.3	3.60	301.5	16.75	5	20	310	2%	224.21	2.77	0.00280
31	60.3	3.60	301.5	16.75	5	20	310	4%	228.92	2.89	0.00193
32	60.3	4.50	301.5	13.40	5	20	310	2%	248.23	2.60	0.00466
33	60.3	4.50	301.5	13.40	5	20	310	4%	255.18	2.94	0.04947
34	60.3	2.90	422.1	20.79	7	20	310	2%	193.65	1.65	0.01743
35	60.3	2.90	422.1	20.79	7	20	310	4%	197.12	2.11	0.01287
36	60.3	3.60	422.1	16.75	7	20	310	2%	206.94	2.23	0.00326
37	60.3	3.60	422.1	16.75	7	20	310	4%	211.03	2.72	0.00964
38	60.3	4.50	422.1	13.40	7	20	310	2%	228.35	2.34	0.00357
39	60.3	4.50	422.1	13.40	7	20	310	4%	236.55	2.69	0.04272
40	60.3	2.90	542.7	20.79	9	20	310	2%	178.63	1.72	0.02559
41	60.3	2.90	542.7	20.79	9	20	310	4%	182.33	1.95	0.02018
42	60.3	3.60	542.7	16.75	9	20	310	2%	196.84	2.05	0.00453
43	60.3	3.60	542.7	16.75	9	20	310	4%	202.21	2.61	0.01423
44	60.3	4.50	542.7	13.40	9	20	310	2%	219.48	2.19	0.01426
45	60.3	4.50	542.7	13.40	9	20	310	4%	225.71	2.18	0.01463

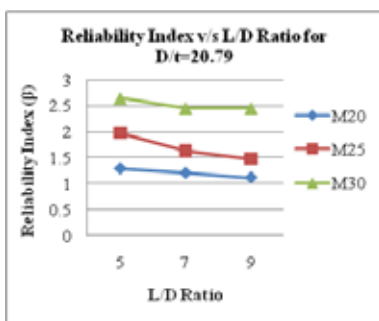


Fig 3.1: Reliability index v/s L/D Ratio for D/t=20.79

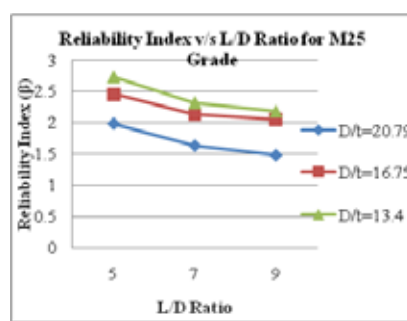


Fig 3.3: Reliability index v/s L/D Ratio for M25 Grade

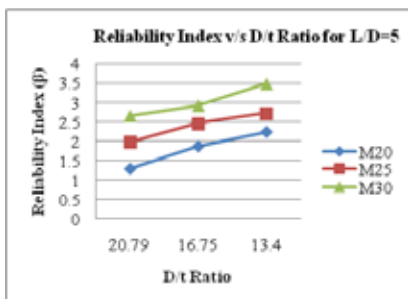


Fig 3.2: Reliability index v/s D/t Ratio for L/D=5

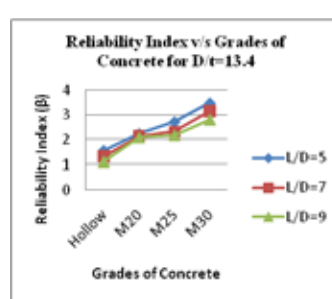


Fig 3.4: Reliability index v/s Grades of Concrete for D/t=13.4

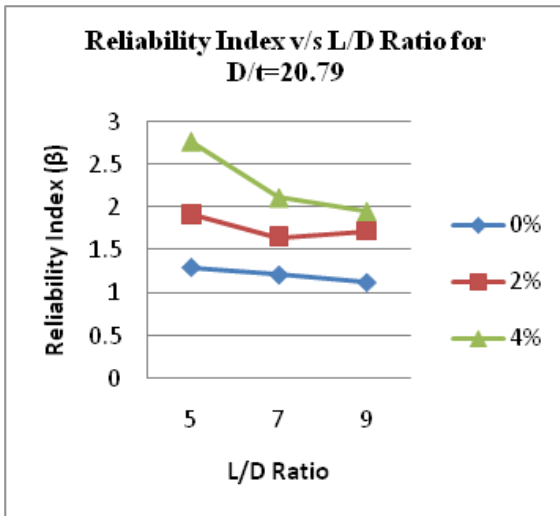


Fig 3.5: Reliability index v/s L/D Ratio for D/t=20.79

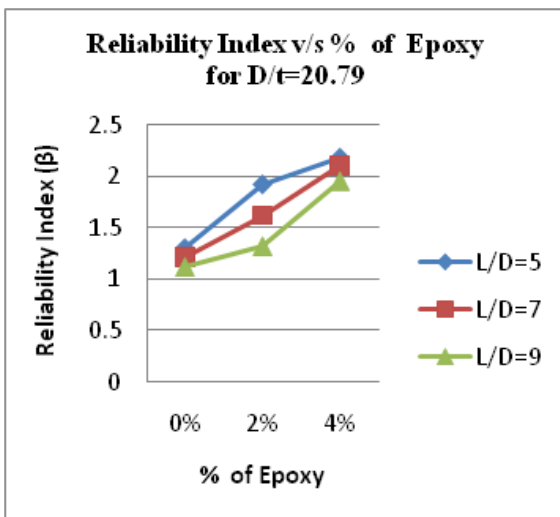


Fig 3.6: Reliability index v/s % of Epoxy for D/t=20.79

#### 4.0 CONCLUSIONS

1. The analytical results obtained using ANSYS software closely match with the experimental results with a difference of about 2.10-6.64%.
2. The ultimate load bearing capacity of CSFT increases with the increase in grade of Concrete for a given L/D value.
3. For a given grade of concrete and a given L/D, the ultimate load carrying capacity increases with decrease in D/t ratio from graph (2.6).
4. For a given grade of concrete and for a given D/t ratio, the ultimate load carrying capacity of CSFT decreases with increase in L/D ratio from graph (2.3).
5. There is a decrease of 5.42% in ultimate load value for M20 and D/t=20.79 for L/D=5 and L/D=9.
6. The reliability index increases with the increase in grade of concrete for a given L/D ratio from graph (3.2).
7. For a given grade of concrete and a given L/D ratio, the reliability index increases with decrease in D/t ratio from graph (3.1).

#### REFERENCE

- 1) Zhijing Ou<sup>1</sup>; Baochun Chen, P.E.2; Kai H. Hsieh<sup>3</sup>; Marvin W. Halling, S.E., F.ASCE<sup>4</sup>; and Paul J. Barr, M.ASCE<sup>5</sup> " Experimental and Analytical Investigation | of Concrete Filled Steel Tubular Columns" | 2) Hsuan-Teh HU<sup>1</sup>, Chiung-Shiann HUANG<sup>2</sup>, Ming-Hsien WU<sup>3</sup> and Yih-Min WU<sup>3</sup> | "Numerical analysis of concrete filled steel tube subjected to axial force | 3) Tengfei XU, Tianyu XIANG\*, Yulin ZHAN, Renda ZHAO " Reliability analysis of | circular concrete-filled steel tube with material and geometrical nonlinearity" | 4) L.H. Han, Concrete-Filled Steel Tubular Structures, Beijing: Science Publishing House, 2000 (in Chinese). | 5) O. Ditlevsen, H.O. Madsen, Structural Reliability Method, New York: John Wiley & Sons, 1996. | 6) R.E. Melchers, Structural Reliability Analysis and Prediction, New York: John Wiley & Sons, Inc, 1999. | 7) H. Haldar, S. Mahadevan, Reliability Assessment Using Stochastic Finite Element | Analysis, New York: John Wiley & Sons, 2000. | 8) P.L. Liu, A.D. Kiureghian, Finite element reliability of geometrical nonlinear uncertain structures, Journal of Engineering Mechanics, 1991, 117(8): 1806-1825. | 9) K. Imai, D.M. Frangopol, Geometrically nonlinear finite element reliability analysis of structural systems, I: theory, Computers and Structures, 2000, 77(6): 677-691. | 10) N. Impollonia, A. Sofi, A response surface approach for the static analysis of stochastic structures with geometrical nonlinearities, Computer Methods in Applied Mechanics and Engineering, 2003, 192(37-38): 4109-4129. | 11) D.M. Frangopol, Y. Ide, E. Spacone, et al., A new look at reliability of reinforced | concrete columns, Structural Safety, 1996, 18(2-3): 123-150. | 12) J.G. Teigen, D.M. Frangopol, S. Sture, et al., Probabilistic FEM for nonlinear concrete structures. I: theory, Journal of Structural Engineering, 1991, 117(9): 2674- 2689 |